HGG Advances

BRIEF COMMUNICATION

Splicing and frameshift variants in *QSER1* may be involved in developmental phenotypes

Megan C. Fischer,[1] Linda M. Reis,[2] Jerica Lenberg,[3] Jennifer Friedman,[3,4] Sarah E. Seese,[2] Sanaa Muheisen,[2] Karin Writzl,[5,6] Barbara Golob,[7] Borut Peterlin,[7] and Elena V. Semina[1,2,8,9,*]

Summary

Human development is a complex process that requires precise control of gene expression through regulatory proteins. Recently, heterozygous variants in *PRR12,* encoding a proline-rich regulatory protein, were found to cause a variable phenotype involving developmental delay/cognitive impairment, neuropsychiatric diagnoses, structural eye anomalies, congenital heart and kidney defects, and poor growth. *QSER1*, encoding glutamine- and serine-rich protein 1, represents a paralog of *PRR12* that shares 28% overall identity at the protein level and stronger conservation (43%) in the C-terminal region. *QSER1* deficiency in human embryonic stem cells causes hypermethylation of many key transcription factor genes, implicating it in the development of multiple organs. Here, we present three unrelated individuals with neurodevelopmental phenotypes, variable other multisystem anomalies, and heterozygous variants in *QSER1*. This includes two novel *de novo* frameshift alleles (p.(Lys1565Argfs*36) and p.(Phe896fs*28)) and one ultra-rare canonical splice site variant resulting in a combination of abnormal transcripts, frameshift (p.(Glu1393Glyfs*26)), and in-frame deletion of a conserved amino acid (p.(Glu1393del)), supported by *in silico* predictions and minigene assays. *In situ* hybridization revealed dynamic and broad expression of *qser1* in zebrafish embryos, including a strong presence in the developing brain. These data suggest a possible role for *QSER1/qser1* in vertebrate development and human disease.

Introduction

Developmental disorders are a broad constellation of conditions characterized by variations from typical human development, including congenital malformations and neurodevelopmental disorders.[1] Variation in genetic factors encoding regulatory proteins that control gene expression via histone modification, chromatin remodeling, and/or binding to specific DNA sequences makes a major contribution to human structural and neurodevelopmental phenotypes.[2] One such gene recently associated with human disease, *PRR12* (MIM: 616633), encodes a proline-rich protein predicted to act as a regulatory cofactor due to its nuclear localization, structure (AT-hook DNA binding domains), and post-translational modification sites.[3] Heterozygous variants (typically loss of function) in *PRR12* cause neurooocular syndrome-1 (MIM: 619539). This syndrome encompasses a broad spectrum of anomalies, with developmental delay/cognitive impairment/neuropsychiatric diagnoses seen in most, along with variable systemic features, including structural eye defects, congenital heart and kidney defects, microcephaly, hypotonia, and failure to thrive.[3–5]

QSER1 (MIM: 619440), encoding glutamine- and serine-rich protein 1, represents a paralog of *PRR12* that has yet to be fully characterized. At the protein level, QSER1 shares 28% identity with PRR12 and shows stronger conservation (43%) in the C-terminal region, called DUF4211 (domain of unknown function).[6] Similar to *PRR12*, *QSER1* displays a broad expression pattern, localizes to the nucleus, and contains post-translational modification sites. One study identified *QSER1* as a novel methylation factor and found that QSER1 cooperates with TET1 to maintain the hypomethylated state of transcriptional and developmental programs, protecting against DNMT3-mediated *de novo* methylation.[7] Consistent with this, *QSER1* knockout in a human embryonic stem cell line showed hypermethylation of genes in many key transcription factor families, including HOX, FOX, GATA, NKX, and PAX, supporting its likely involvement in the development of multiple organs.[7] However, a role for *QSER1* in human disease remains to be uncovered. Several studies identified a possible association between *QSER1* and various human phenotypes, including coronary artery disease,[8] inguinal hernia,[9] and neurodevelopmental phenotypes.[10–15] Another recent study showed

[1]Department of Cell Biology, Neurobiology and Anatomy, Medical College of Wisconsin, Milwaukee, WI 53226, USA; [2]Department of Ophthalmology and Visual Sciences, Medical College of Wisconsin, Milwaukee, WI 53226, USA; [3]Rady Children's Institute for Genomic Medicine, Rady's Children's Hospital, San Diego, CA 92123, USA; [4]Departments of Neuroscience and Pediatrics, University of California San Diego, and Rady Children's Hospital Division of Neurology, San Diego, CA 92123, USA; [5]Clinical Institute of Genomic Medicine, University Medical Center Ljubljana, 1000 Ljubljana, Slovenia; [6]Faculty of Medicine, University of Ljubljana, 1000 Ljubljana, Slovenia; [7]Centre for Mendelian Genomics, Clinical Institute of Genomic Medicine, University Medical Center Ljubljana, Šlajmerjeva 4, 1000 Ljubljana, Slovenia; [8]Department of Pediatrics and Children's Research Institute, Medical College of Wisconsin and Children's Wisconsin, Milwaukee, WI 53226, USA
[9]Lead contact
*Correspondence: esemina@mcw.edu
https://doi.org/10.1016/j.xhgg.2025.100539.

that *QSER1* functions as an anti-apoptotic factor.[16] Several reports have demonstrated that its upregulation is associated with poor outcomes in multiple cancers, and widespread expression in adult tissues has been reported.[17–19]

Here, we present three individuals with developmental phenotypes and novel or ultra-rare heterozygous variants in *QSER1*, along with evidence of embryonic expression of zebrafish *qser1*, suggesting its possible role in development and disease.

Material and methods

Study cohort, ES, and variant analyses

This study was approved by the institutional review boards of the Medical College of Wisconsin and the University of Iowa (individual 1), with written informed consent obtained for every participant. Additional individuals with *QSER1* variants were identified through matchmaker databases with local study approval and/or consent to publish. Genomic DNA was collected from individual 1 and his mother utilizing standard procedures. Sanger sequencing of *PITX2* and *FOXC1* was completed as previously described,[20] and samples were submitted for exome sequencing (ES) to Psomagen (Rockville, MD) and processed using standard bioinformatic pipelines (supplemental methods). Individuals 2 and 3 were identified through GeneMatcher.[21]

Variant evaluation and scoring were carried out in accordance with the criteria put forth by the American College of Medical Genetics/Association for Molecular Pathology[22] using recently published updated *in silico* score guidelines.[23] Variants from all individuals were annotated with GERP++ scores[24] using VarSeq (Golden Helix). Potential splicing effects were investigated using the SpliceAI Lookup tool from the Broad Institute, which provides scores for SpliceAI[25] and Pangolin.[26] Further *in vitro* RNA analysis was conducted for the c.4178-2A>G variant to verify these predictions via a minigene assay (supplemental methods).

Identification of zebrafish *qser1* and expression studies

All zebrafish work was approved by the Institutional Animal Care and Use Committee at the Medical College of Wisconsin, and zebrafish were maintained using standard protocols.[27] *In situ* hybridization was performed for *qser1* as previously described[27] on zebrafish whole-mount embryos and sections at 24, 48, 72, and 120 h post-fertilization (hpf) using an RNAscope Probe (catalog no. 1273391-C1, Advanced Cell Diagnostics, Newark, CA) that targets nucleotides 411–1,329 of zebrafish *qser1* (XM_005169967.4) (supplemental methods). Human QSER1 (NP_001070254.2) and zebrafish qser1 (XP_005170024.1) protein sequences were aligned using the European Molecular Biology Laboratory-European Bioinformatics Institute Clustal Omega MSA tool (CLUSTAL 0(1.2.4)).[28] Percent identity was calculated using NCBI protein BLAST, and protein domains were annotated via UniProt.

Results

Identification of *QSER1* variants in individuals with complex phenotypes

Novel or ultra-rare variants in *QSER1* were identified in three unrelated individuals with complex phenotypes (Figures 1A and S1; Table 1). The variants affect exons 4, 5, and 7 of *QSER1* (NM_001076786.3), which are included in all five of the known RefSeq transcripts from NCBI (Figure 1B; Table 2). The *QSER1* gene shows strong constraint against loss of function with a probability of loss-of-function intolerance of 1.0 and a loss-of-function observed/expected upper bound fraction of 0.35 (gnomAD version 4.1.0).

Individual 1 is a 12-year-old male, born at 25.5 weeks by emergency cesarean section due to maternal hypertension/preeclampsia, with a clinical diagnosis of Axenfeld-Rieger syndrome (ARS) (Figure 1A). He had ocular findings consistent with Axenfeld-Rieger anomaly, including bilateral posterior embryotoxon in the peripheral cornea, moderately high myopic astigmatism, mild iris hypoplasia, and anisocoria. Syndromic features included cone-shaped teeth, hypospadias, inguinal hernia, bilateral 2–3 syndactyly of the toes, early delays in speech and fine motor skills, learning difficulties requiring specialized schooling, and psychiatric/behavioral issues, including attention-deficit/hyperactivity disorder, depression, and impulse control disorder, requiring in-patient treatment. His growth parameters were in the normal range and facies were non-dysmorphic. Additional neonatal complications included bronchopulmonary dysplasia, respiratory distress syndrome, retinopathy of prematurity (at 3 months of age) and patent ductus arteriosus (PDA), which are likely attributable to prematurity. A comprehensive analysis of ARS genes was negative. Duo ES analysis of the proband and mother (father not available) was negative for any pathogenic or likely pathogenic variants in known disease genes but identified two variants of interest: a heterozygous splicing variant (c.4178-2A>G) in *QSER1* and a hemizygous missense variant (NM_001368397.1:c.62G>A, p.(Gly21Asp); hg19 chrX:12516819) in *FRMPD4* (MIM: 300838). Hemizygous loss-of-function variants in *FRMPD4* are associated with X-linked intellectual developmental disorder 104 and/or epilepsy (XLID104 [MIM: 300983]), which potentially overlaps the observed neurodevelopmental phenotype. The variant was not present in the mother, has indeterminate *in silico* scores (REVEL = 0.304, AlphaMissense = 0.782), is present in a public database (gnomAD version 4.1.0) in a hemizygote (×1), and falls outside of known domains in a region without other pathogenic variants.[29] The *QSER1* variant was present in the proband (19/32 reads), not present in the mother (Figure S1), and observed in only 3/1,596,730 individuals in a public database (gnomAD version4.1.0). The variant disrupts a canonical splice acceptor site (AG) and is strongly predicted to disrupt splicing by SpliceAI and Pangolin (Table 2). This variant is located just before exon 5 and is predicted to lead to the loss of a splice acceptor site by both algorithms (Δ = 1 and 0.9, respectively). With no acceptor gain, this would lead to skipping of the 323-bp exon 5, resulting in frameshift with early truncation (p.(Glu1393Glyfs*26)) due to a novel stop codon in exon 6 (of 13), and would be expected

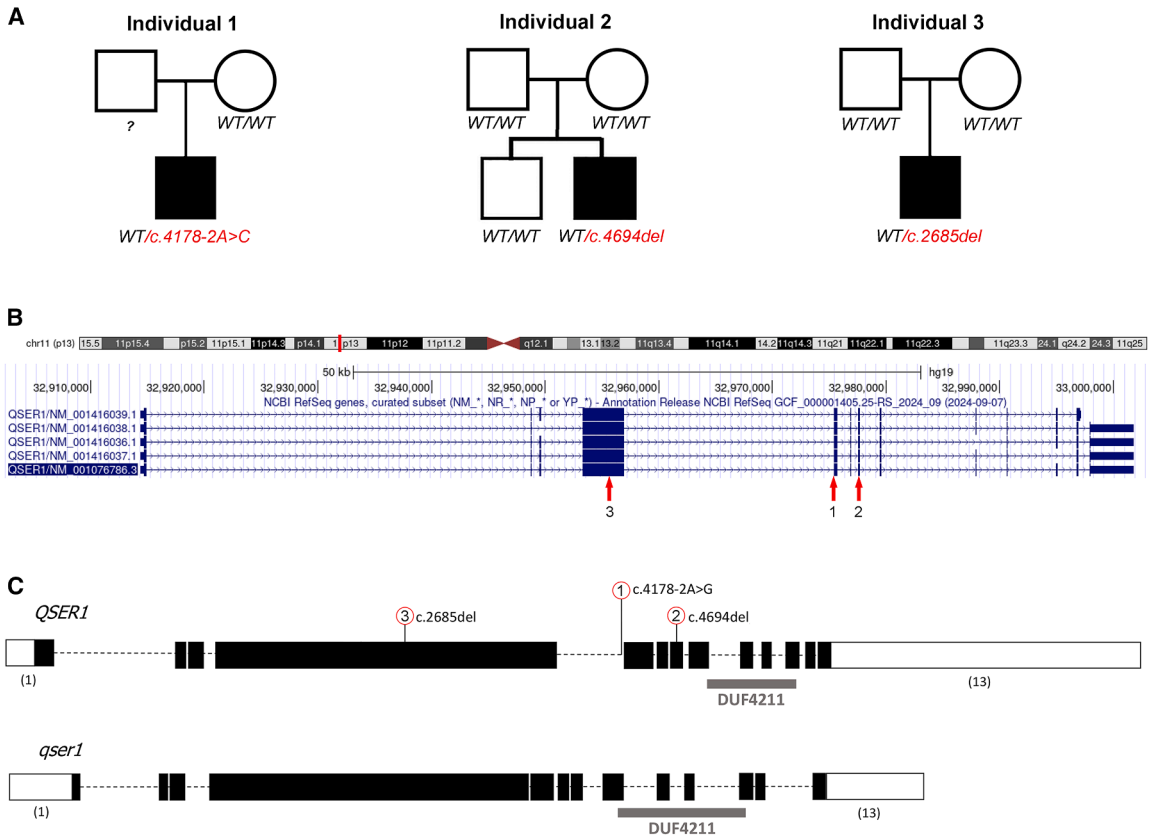

Figure 1. Positions and inheritance of the identified heterozygous *QSER1* variants

(A) Pedigrees and genotypic data for the affected individuals 1, 2, and 3 and their families. Solid symbol indicates affected; empty symbol indicates unaffected. Genetic data noted under each individual. WT, wild type; ?, not tested.

(B) Genome Browser view of human *QSER1* isoforms with positions of variants identified in individuals 1–3 denoted with red arrows.

(C) Schematics of human *QSER1* (NM_001076786.3) and zebrafish *qser1* (XM_005169967.5) showing similar gene structure. Black boxes represent the coding sequence and white boxes the untranslated portions of the exons. The position of the DUF4211 domain is indicated with a gray rectangle, the location of human variants is indicated with red circles above the human gene, and the numbers in parentheses denote the first and last exon.

to be subject to nonsense-mediated decay (NMD). Both algorithms also have a weaker, but significant, prediction for a splice acceptor gain ($\Delta = 0.59$ and 0.74). This would instead lead to a 3-bp deletion at the start of exon 5, resulting in an in-frame deletion that removes one amino acid (aa) from the protein (p.(Glu1393del)); the GERP++ score (5.7) indicates that Glu1393 is a highly conserved residue with no aa substitutions at this position present in a general population database (gnomAD version 4.1.0). A minigene assay was designed to test the effects of this variant on splicing (Figure S2; supplemental methods). When expressed in B3 human lens epithelial cells (HLE-B3), the mutant minigene produced an upper band (838 bp) of similar size to wild type; however, sequencing revealed it to be the in-frame 3-bp deletion leading to p.(Glu1393del), and a unique lower band (518 bp) that sequencing revealed to be the predicted frameshift (due to exon 5 skipping) resulting in p.(Glu1393Glyfs*26). Control sample (untransfected HLE-B3 cells) showed robust endogenous *QSER1* expression (Figure S2).

Individual 2 is a 3-year-old male, born at 40 weeks with unilateral congenital sensorineural hearing loss (Figure 1A). Additional features include mild right-sided spastic hemiparesis (inconsistently observed), bilateral ankle clonus (right > left), history of frequent falls, toe walking, disordered breathing during sleep, hyperkinetic tongue movements, ventricular septal defect, and ocular anomalies (amblyopia and anisometropia with myopia). Height and weight are in the normal range, but head circumference shows borderline microcephaly (4^{th} percentile); facies were otherwise non-dysmorphic. Brain MRI was limited by artifact from the right cochlear nerve implant but showed unilateral hypoplasia of the cochlear nerve, stable enlarged right aqueduct, and mild asymmetric dilation of the right vestibule. Quad genome sequencing analysis identified a heterozygous *de novo* variant (c.4694del) in *QSER1* that leads to frameshift (p.(Lys1565Argfs*36)) and is predicted to undergo NMD. The variant was present in the proband and absent in both parents (Figure S1), the male unaffected sibling, and control databases (Table 2).

Individual 3 is a 1-year-old male with a congenital heart defect (large atrial septal defect secundum, PDA, and dysplastic pulmonary valve based on ultrasound), preaxial polydactyly of the right thumb with duplication of both

Table 1. Phenotypic findings in the presented individuals with associated HPO terms

	HPO term	Individual 1	Individual 2	Individual 3
Age	–	12 years 11 months	3 years	1 year
Gender	–	male	male	male
Race/ethnicity	–	White	White	White
Height	–	162.0 cm (75th percentile) ($Z = +1.0$)	102.4 cm (75th percentile) ($Z = +0.65$)	65 cm (<5th percentile)[a] ($Z = -4.4$)
Weight	–	66.1 kg (95th percentile) ($Z = +1.72$)	15.7 kg (50th percentile) ($Z = +0.1$)	7.7 kg (10th percentile)[a] ($Z = -2.0$)
Head circumference	–	55.1 cm (50th–75th percentile) ($Z = +0.68$)	48.5 cm (<5th percentile) ($Z = -1.72$)	42.5 cm (5th percentile)[a] ($Z = -2.7$)
Nervous system/neurodevelopmental				
Neurodevelopmental delay	HP:0012758	X	–	X
Atypical behavior	HP:0000708	X	–	NA
Depression	HP:0000716	X	–	NA
Attention-deficit/hyperactivity disorder	HP:0007018	X	–	NA
Frequent falls	HP:0002359	–	X	NA
Gait disturbance	HP:0001288	–	X	NA
Spastic hemiparesis	HP:0011099	–	mild, right sided	NA
Ankle clonus	HP:0011448	–	B (right > left)	NA
Sleep-related breathing disorders	HP:5200283	–	X	NA
Tongue fasciculations	HP:0001308	–	X	NA
Hypertonia	HP:0001276	–	–	X
Ocular				
Amblyopia	HP:0000646	–	X	–
Anisocoria	HP:0009916	mild	–	–
Anisometropia	HP:0012803	–	X	–
Astigmatism	HP:0000483	X	–	–
Hypoplasia of the iris	HP:0007676	mild	–	–
Myopia	HP:0000545	X	X	–
Posterior embryotoxon	HP:0000627	B	–	–
Retinopathy of prematurity	HP:0500049	X[b]	–	X[b]
Dental				
Conical teeth	HP:0000698	X	–	NA
Dysmorphic features				
Prominent forehead	HP:0011220	–	–	X
Hypertelorism	HP:0000316	–	–	X
Posteriorly rotated ears	HP:0000358	–	–	X
Limb/musculoskeletal anomalies				
2–3 toes syndactyly	HP:0004691	X	–	–
Duplication of thumb phalanx	HP:0009942	–	–	right
Cardiovascular				
Abnormal heart morphology	HP:0001627	–	X	X
Atrial septal defect	HP:0001631	–	–	X

(*Continued on next page*)

Table 1. ***Continued***

	HPO term	Individual 1	Individual 2	Individual 3
Ventricular septal defect	HP:0001629	–	X	–
Patent ductus arteriosus after premature birth	HP:0011649	X[b]	–	X[b]
Dysplastic pulmonary valve	HP:0005164	–	–	X
Genitourinary				
Hypospadias	HP:0000047	X	–	–
Cryptorchidism	HP:0000028	–	–	B
Inguinal hernia	HP:0000023	B	–	B
Other				
Appendicitis	HP:6000143	OP at 5 years	–	–
Nasogastric tube feeding	HP:0040288	–	–	X
Neonatal respiratory distress	HP:0002643	X[b]	–	X[b]
Congenital sensorineural hearing impairment	HP:0008527	–	X	–
Brain imaging abnormality	HP:0410263	NA	X	X
Premature birth	HP:0001622	25 weeks EGA	–	24 weeks EGA

B, bilateral; EGA, estimated gestational age; HPO, Human Phenotype Ontology; NA, not applicable; OP, operation; X, present; –, not present.
[a]Percentiles given for adjusted age due to premature birth.
[b]Features likely attributable to prematurity.

phalanges on the right hand, bilateral inguinal hernia, and undescended testes (Figure 1A). Neurological examination identified limb hypertonia with brisk tendon reflexes, decreased eye contact, and significant developmental delay (not able to sit independently, decreased spontaneous movements). Other clinical details include prematurity (born at 24 weeks' gestation by emergency cesarean section due to maternal preeclampsia and intrauterine growth restriction, with Apgar scores 3/4/6 and birth weight/length/head circumference at 380 g/27 cm/20 cm. At 1 year, growth parameters remained low, even corrected for gestational age, and dysmorphic features included prominent forehead, hypertelorism and low-set posteriorly rotated ears. Bronchopulmonary dysplasia and retinopathy of prematurity (stage 3; treated with laser photocoagulation and later bilateral vitrectomy) with horizontal nystagmus were also present and are well-established complications of prematurity. Brain MRI showed changes consistent with periventricular leukomalacia and signs of previous microbleeds in the brain parenchyma. His family history is negative. Trio ES analysis identified a *de novo* heterozygous frameshift variant (c.2685del p.(Phe896fs*28)) in *QSER1* predicted to undergo NMD. The variant was absent in both parents and control databases (Table 2; Figure S1).

Zebrafish *qser1* shows broad expression during zebrafish development

A single zebrafish ortholog, *qser1*, located on chromosome 18, has been identified with a distinct transcript (XM_005169967.5). The gene shows conserved overall structure (Figure 1C) and encodes a protein of 1,708 aa (vs. 1,864 aa in humans). Zebrafish qser1 shows 43% overall identity with human QSER1 at the protein level, with stronger conservation (59.02%) of the only annotated DUF (DUF4211) (Figure S3). This conserved C-terminal region would be absent in the truncated proteins encoded by the frameshift transcripts if they escape NMD, but it would be intact in the in-frame deletion transcript additionally associated with the splicing variant in individual 1.

To determine the developmental expression of *qser1*, we performed *in situ* hybridization on whole zebrafish embryos and transverse sections at 24, 48, 72, and 120 hpf, with a minimum of 5 embryos at each time point. The *qser1* transcripts were detected at all tested embryonic stages and show a broad expression pattern (Figure 2). Strong *qser1* expression was detected across multiple developing brain regions, including the forebrain (diencephalon, telencephalon), optic tectum and tegmentum, and cerebellum at 24 (Figure 2A), 48 (Figure 2B), and 120 hpf (Figures 2G and 2H). In the developing eye, *qser1* expression was detected in the anterior segment (lens, cornea) and the retina, with diffuse expression at 48 hpf (Figure 2C) and stronger expression in the inner and outer nuclear layers at later stages (Figures 2D–2G); enrichment in the ciliary marginal zone was seen at all stages (Figures 2C–2G). Expression was also seen in the pharyngeal arches (Figures 2A and 2B), the otic vesicle (Figures 2A and 2B), the gastrointestinal tract (Figure 2I), and the fins (Figures 2B and 2I).

Table 2. Variants in *QSER1* and their characteristics

	Individual 1	Individual 2	Individual 3
Genomic coordinates (hg19)	chr11:32975401	chr11:32977609	chr11:32955487
Exon/intron	intron 4–5	exon 7	exon 4
cDNA NC_000011.10 (NM_001076786.3)	c.4178-2A>G	c.4694del	c.2685del
Protein (NP_001070254.2)	p.(Glu1393Glyfs*26) and/or p.(Glu1393del)	p.(Lys1565Argfs*36)	p.(Phe896fs*28)
Zygosity	heterozygous	heterozygous	heterozygous
Inheritance	NP in mother, father NA	*de novo*	*de novo*
gnomAD version 4.1.0 frequency	3/1596730	absent	absent
***In silico* predictors**			
GERP++	5.7	NA	NA
SpliceAI (Δ > 0.1)	acceptor loss (1.0) acceptor gain (0.59)	–	–
Pangolin (Δ > 0.1)	acceptor loss (0.9) acceptor gain (0.74)	acceptor loss (0.05) acceptor gain (0.03)	splice loss (0.05)

NA, not available; NP, not present.

Discussion

This study reports two novel *de novo* frameshift alleles and one ultra-rare splicing variant in *QSER1* in individuals with complex developmental phenotypes. All frameshift transcripts are predicted to be degraded by NMD; however, if stable, then the encoded proteins would be expected to be severely truncated and lack the conserved DUF4211 domain. The splicing allele is predicted and verified by minigene assays to result in two transcripts, frameshift (also prior to DUF4211) and in-frame deletion of a conserved aa. The main overlapping features observed in all three individuals are neurodevelopmental phenotypes. There is a wide variety of other systemic anomalies, including ocular, cardiovascular, limb, craniofacial/hearing loss, and genitourinary defects. Extreme prematurity was noted in two individuals and represents a clear confounding factor, but it does not rule out a possible contribution from the *QSER1* deficiency. Furthermore, review of the Human Gene Mutation Database (HGMD Professional 2024.4) identified other published *de novo* variants in *QSER1* in large autism/developmental disorder cohorts without further phenotypic details,[10–14] including six missense variants, one in-frame deletion, and one nonsense variant, all prior to the DUF4211 domain, as well as a *de novo* missense variant in a single proband with schizophrenia but without developmental delay.[15] These data support the possible involvement of *QSER1* in neurological phenotypes.

Current expression data of human or mouse *QSER1*/*Qser1* are limited to publicly available datasets. The Human Protein Atlas[18] and BioGPS[19] show ubiquitous *QSER1* expression in adult human tissues. The mouse ortholog *Qser1* shows broad expression, with the highest enrichment in ocular tissues.[19] The data presented here demonstrate widespread expression of *qser1* during zebrafish development, with a strong presence in the developing brain, consistent with the observed neurological features, as well as other sites (eye, otic vesicle, fins [limbs]) variably affected in the described individuals. Expression was not detected in cardiovascular or genitourinary structures, affected in some individuals; however, it is important to acknowledge that the sensitivity of the methods and the developmental time points examined may not have been sufficient to capture all relevant expression. Review of developmental zebrafish expression in Daniocell shows enrichment of *qser1* in neural and mesenchymal cell clusters, with some expression in almost all clusters, including heart (myocardium) and kidney (pronephros), supporting its possible role in the development of those systems. Expression of *qser1* also shows an interesting overlap with its paralogs *prr12a* and *prr12b*, which both show broad expression in the brain and eye, but did not show heart or kidney expression despite the presence of heart and kidney anomalies in individuals with variants in *PRR12*.[6] These data support a role for *qser1* in embryonic development; however, further studies into the developmental expression of *QSER1/Qser1/qser1* in humans and other vertebrate species are needed.

This study presents *QSER1* as a candidate gene for human disease, but the specific contribution remains uncertain due to small cohort size and phenotypic variability. The high degree of the observed phenotypic variation could be explained by the presence of other variants within the larger regulatory network modifying the effects of *QSER1* deficiency in different tissues. Further investigations into the function of the gene and identification of additional individuals with damaging variants in this

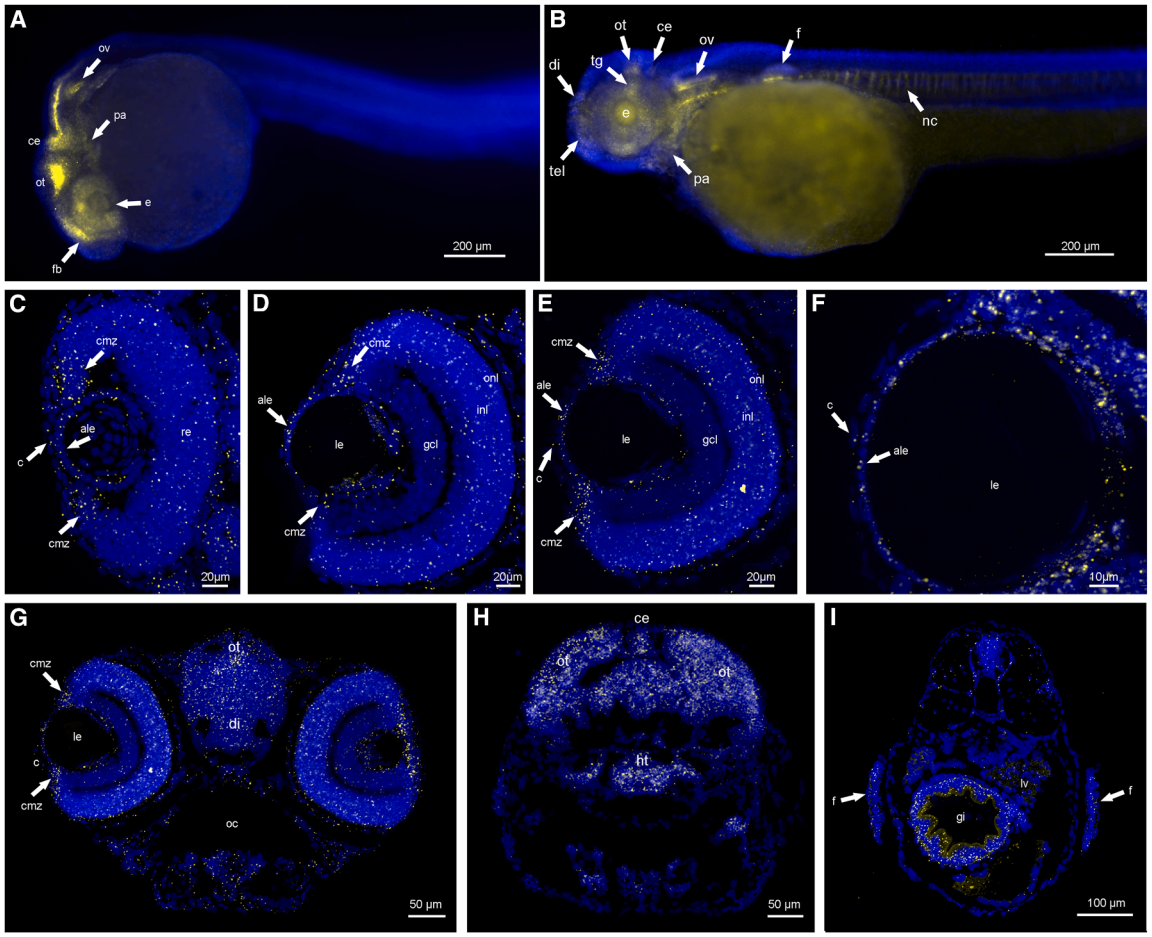

Figure 2. Embryonic expression of zebrafish *qser1*

Zebrafish *qser1* expression during embryonic development at 24 (A), 48 (B–D), 72 (E and F), and 120 hpf (G–I). Anteroposterior view of laterally positioned whole-mount embryos (A and B) and transverse paraffin sections (C–I) oriented dorsoventrally. A scale bar indicating the magnification is shown in the bottom right corner. ale, anterior lens epithelium; c, cornea; ce, cerebellum; cmz, ciliary marginal zone; di, diencephalon; e, eye; f, fin; fb, forebrain; gi, gastrointestinal tract; gcl, ganglion cell layer; ht, hypothalamus; inl, inner nuclear layer; le, lens; lv, liver; nc, notochord; oc, oral cavity; onl, outer nuclear layer; ot, optic tectum; ov, otic vesicle; pa, pharyngeal arches; re, retina; tg, optic tegmentum; tel, telencephalon.

gene will be needed to fully understand its possible contribution to human development and disease.

Data and code availability

QSER1 variants were deposited in ClinVar (ClinVar: SCV006310942, ClinVar: SCV006310943, and ClinVar: SCV006310944).

Acknowledgments

The authors gratefully acknowledge the individuals and their families for their participation in research studies and the CRI Histology Facility for assistance with histology. This work was supported by National Eye Institute grant no. R01EY015518 (E.V.S.), as well as by funds provided by the Children's Research Institute Foundation at Children's Wisconsin (E.V.S.).

Declaration of interests

The authors declare no competing interests.

Supplemental information

Supplemental information can be found online at https://doi.org/10.1016/j.xhgg.2025.100539.

Web resources

BioGPS, https://biogps.org/
Daniocell, https://daniocell.nichd.nih.gov/
GnomAD, https://gnomad.broadinstitute.org/
Human Gene Mutation Database (HGMD), https://my.qiagendigitalinsights.com/bbp/view/hgmd/pro/start.php
Human Phenotype Ontology (HPO), https://hpo.jax.org/
Human Protein Atlas (HPA), https://www.proteinatlas.org/
NCBI Protein BLAST, https://blast.ncbi.nlm.nih.gov/Blast.cgi
Online Mendelian Inheritance in Man (OMIM), https://www.omim.org/
SpliceAI Lookup, https://spliceailookup.broadinstitute.org/
UniProt, https://www.uniprot.org/
University of California, Santa Cruz (UCSC) Genome Browser, https://genome.ucsc.edu/index.html
ZFIN, https://zfin.org/

Received: May 25, 2025
Accepted: October 23, 2025

References

1. Deciphering Developmental Disorders Study (2015). Large-scale discovery of novel genetic causes of developmental disorders. Nature *519*, 223–228. https://doi.org/10.1038/nature14135.
2. Zug, R. (2022). Developmental disorders caused by haploinsufficiency of transcriptional regulators: a perspective based on cell fate determination. Biol. Open *11*, bio058896. https://doi.org/10.1242/bio.058896.
3. Leduc, M.S., McGuire, M., Madan-Khetarpal, S., Ortiz, D., Hayflick, S., Keller, K., Eng, C.M., Yang, Y., and Bi, W. (2018). De novo apparent loss-of-function mutations in PRR12 in three patients with intellectual disability and iris abnormalities. Hum. Genet. *137*, 257–264. https://doi.org/10.1007/s00439-018-1877-0.
4. Chowdhury, F., Wang, L., Al-Raqad, M., Amor, D.J., Baxová, A., Bendová, Š., Biamino, E., Brusco, A., Caluseriu, O., Cox, N.J., et al. (2021). Haploinsufficiency of PRR12 causes a spectrum of neurodevelopmental, eye, and multisystem abnormalities. Genet. Med. *23*, 1234–1245. https://doi.org/10.1038/s41436-021-01129-6.
5. Reis, L.M., Costakos, D., Wheeler, P.G., Bardakjian, T., Schneider, A., Fung, S.S.M., and Semina, E.V. (2021). Dominant variants in PRR12 result in unilateral or bilateral complex microphthalmia. Clin. Genet. *99*, 437–442. https://doi.org/10.1111/cge.13897.
6. Musco, A., Martini, D., Digregorio, M., Broccoli, V., and Andreazzoli, M. (2024). Shedding a Light on Dark Genes: A Comparative Expression Study of PRR12 Orthologues during Zebrafish Development. Genes *15*, 492. https://doi.org/10.3390/genes15040492.
7. Dixon, G., Pan, H., Yang, D., Rosen, B.P., Jashari, T., Verma, N., Pulecio, J., Caspi, I., Lee, K., Stransky, S., et al. (2021). QSER1 protects DNA methylation valleys from de novo methylation. Science *372*, eabd0875. https://doi.org/10.1126/science.abd0875.
8. Hariharan, P., and Dupuis, J. (2021). Mapping gene and gene pathways associated with coronary artery disease: a CARDIoGRAM exome and multi-ancestry UK biobank analysis. Sci. Rep. *11*, 16461. https://doi.org/10.1038/s41598-021-95637-9.
9. Wei, J., Attaar, M., Shi, Z., Na, R., Resurreccion, W.K., Haggerty, S.P., Zheng, S.L., Helfand, B.T., Ujiki, M.B., and Xu, J. (2022). Identification of fifty-seven novel loci for abdominal wall hernia development and their biological and clinical implications: results from the UK Biobank. Hernia *26*, 335–348. https://doi.org/10.1007/s10029-021-02450-4.
10. Jiao, J., Zhang, M., Yang, P., Huang, Y., Hu, X., Cai, J., Yang, C., Situ, M., Zhang, H., Fu, L., et al. (2020). Identification of De Novo JAK2 and MAPK7 Mutations Related to Autism Spectrum Disorder Using Whole-Exome Sequencing in a Chinese Child and Adolescent Trio-Based Sample. J. Mol. Neurosci. *70*, 219–229. https://doi.org/10.1007/s12031-019-01456-z.
11. Turner, T.N., Wilfert, A.B., Bakken, T.E., Bernier, R.A., Pepper, M.R., Zhang, Z., Torene, R.I., Retterer, K., and Eichler, E.E. (2019). Sex-Based Analysis of De Novo Variants in Neurodevelopmental Disorders. Am. J. Hum. Genet. *105*, 1274–1285. https://doi.org/10.1016/j.ajhg.2019.11.003.
12. Kaplanis, J., Samocha, K.E., Wiel, L., Zhang, Z., Arvai, K.J., Eberhardt, R.Y., Gallone, G., Lelieveld, S.H., Martin, H.C., McRae, J.F., et al. (2020). Evidence for 28 genetic disorders discovered by combining healthcare and research data. Nature *586*, 757–762. https://doi.org/10.1038/s41586-020-2832-5.
13. Fu, J.M., Satterstrom, F.K., Peng, M., Brand, H., Collins, R.L., Dong, S., Wamsley, B., Klei, L., Wang, L., Hao, S.P., et al. (2022). Rare coding variation provides insight into the genetic architecture and phenotypic context of autism. Nat. Genet. *54*, 1320–1331. https://doi.org/10.1038/s41588-022-01104-0.
14. Zhou, X., Feliciano, P., Shu, C., Wang, T., Astrovskaya, I., Hall, J.B., Obiajulu, J.U., Wright, J.R., Murali, S.C., Xu, S.X., et al. (2022). Integrating de novo and inherited variants in 42,607 autism cases identifies mutations in new moderate-risk genes. Nat. Genet. *54*, 1305–1319. https://doi.org/10.1038/s41588-022-01148-2.
15. Guipponi, M., Santoni, F.A., Setola, V., Gehrig, C., Rotharmel, M., Cuenca, M., Guillin, O., Dikeos, D., Georgantopoulos, G., Papadimitriou, G., et al. (2014). Exome sequencing in 53 sporadic cases of schizophrenia identifies 18 putative candidate genes. PLoS One *9*, e112745. https://doi.org/10.1371/journal.pone.0112745.
16. Zhao, X., Fang, K., Liu, X., Yao, R., Wang, M., Li, F., Hao, S., He, J., Wang, Y., Fan, M., et al. (2023). QSER1 preserves the suppressive status of the pro-apoptotic genes to prevent apoptosis. Cell Death Differ. *30*, 779–793. https://doi.org/10.1038/s41418-022-01085-x.
17. Wu, M., Shi, Q.M., Duan, S.L., Ou-Yang, D.J., Chen, P., Tu, B., and Huang, P. (2022). Insights into the Association Between QSER1 and M2 Macrophages and Remarkable Malignancy Characteristics in Hepatocellular Carcinoma. Int. J. Gen. Med. *15*, 1765–1775. https://doi.org/10.2147/IJGM.S352574.
18. Thul, P.J., Akesson, L., Wiking, M., Mahdessian, D., Geladaki, A., Ait Blal, H., Alm, T., Asplund, A., Bjork, L., Breckels, L.M., et al. (2017). A subcellular map of the human proteome. Science *356*, eaal3321. https://doi.org/10.1126/science.aal3321.
19. Wu, C., Orozco, C., Boyer, J., Leglise, M., Goodale, J., Batalov, S., Hodge, C.L., Haase, J., Janes, J., Huss, J.W., 3rd, and Su, A.I. (2009). BioGPS: an extensible and customizable portal for querying and organizing gene annotation resources. Genome Biol. *10*, R130. https://doi.org/10.1186/gb-2009-10-11-r130.
20. Reis, L.M., Tyler, R.C., Volkmann Kloss, B.A., Schilter, K.F., Levin, A.V., Lowry, R.B., Zwijnenburg, P.J.G., Stroh, E., Broeckel, U., Murray, J.C., and Semina, E.V. (2012). PITX2 and FOXC1 spectrum of mutations in ocular syndromes. Eur. J. Hum. Genet. *20*, 1224–1233. https://doi.org/10.1038/ejhg.2012.80.
21. Sobreira, N., Schiettecatte, F., Valle, D., and Hamosh, A. (2015). GeneMatcher: a matching tool for connecting investigators with an interest in the same gene. Hum. Mutat. *36*, 928–930. https://doi.org/10.1002/humu.22844.
22. Richards, S., Aziz, N., Bale, S., Bick, D., Das, S., Gastier-Foster, J., Grody, W.W., Hegde, M., Lyon, E., Spector, E., et al. (2015). Standards and guidelines for the interpretation of sequence variants: a joint consensus recommendation of the American College of Medical Genetics and Genomics and the Association for Molecular Pathology. Genet. Med. *17*, 405–424. https://doi.org/10.1038/gim.2015.30.
23. Bergquist, T., Stenton, S.L., Nadeau, E.A.W., Byrne, A.B., Greenblatt, M.S., Harrison, S.M., Tavtigian, S.V., O'Donnell-Luria, A., Biesecker, L.G., Radivojac, P., et al. (2025). Calibration of additional computational tools expands ClinGen recommendation options for variant classification with

PP3/BP4 criteria. Genet. Med. *27*, 101402. https://doi.org/10.1016/j.gim.2025.101402.

24. Davydov, E.V., Goode, D.L., Sirota, M., Cooper, G.M., Sidow, A., and Batzoglou, S. (2010). Identifying a high fraction of the human genome to be under selective constraint using GERP++. PLoS Comput. Biol. *6*, e1001025. https://doi.org/10.1371/journal.pcbi.1001025.
25. Jaganathan, K., Kyriazopoulou Panagiotopoulou, S., McRae, J.F., Darbandi, S.F., Knowles, D., Li, Y.I., Kosmicki, J.A., Arbelaez, J., Cui, W., Schwartz, G.B., et al. (2019). Predicting Splicing from Primary Sequence with Deep Learning. Cell *176*, 535–548.e24. https://doi.org/10.1016/j.cell.2018.12.015.
26. Zeng, T., and Li, Y.I. (2022). Predicting RNA splicing from DNA sequence using Pangolin. Genome Biol. *23*, 103. https://doi.org/10.1186/s13059-022-02664-4.
27. Seese, S.E., Deml, B., Muheisen, S., Sorokina, E., and Semina, E.V. (2021). Genetic disruption of zebrafish mab21l1 reveals a conserved role in eye development and affected pathways. Dev. Dyn. *250*, 1056–1073. https://doi.org/10.1002/dvdy.312.
28. Madeira, F., Madhusoodanan, N., Lee, J., Eusebi, A., Niewielska, A., Tivey, A.R.N., Lopez, R., and Butcher, S. (2024). The EMBL-EBI Job Dispatcher sequence analysis tools framework in 2024. Nucleic Acids Res. *52*, W521–W525. https://doi.org/10.1093/nar/gkae241.
29. Li, R.K., Li, H., Tian, M.Q., Li, Y., Luo, S., Liang, X.Y., Liu, W.H., Li, B.M., Shi, X.Q., Li, J., et al. (2024). Investigation of FRMPD4 variants associated with X-linked epilepsy. Seizure *116*, 45–50. https://doi.org/10.1016/j.seizure.2023.05.014.